MAPAN-Journal of Metrology Society of India (December 2020) 35(4):491–498
https://doi.org/10.1007/s12647-020-00393-2

ORIGINAL PAPER

Realization of the New Kilogram Using ^{28}Si-Enriched Spheres and Dissemination of Mass Standards at NMIJ

N. Kuramoto*, S. Mizushima, L. Zhang, K. Fujita, Y. Ota, S. Okubo and H. Inaba

National Metrology Institute of Japan, National Institute of Advanced Industrial Science and Technology, 1-1-1 Umezono, Tsukuba, Ibaraki 305-8563, Japan

Received: 27 June 2020 / Accepted: 13 August 2020 / Published online: 23 September 2020

Abstract: The new definition of the kilogram was implemented on May 20, 2019. The kilogram is presently defined by a fixed value of the Planck constant. On the basis of the new definition, the kilogram will be realized at the National Metrology Institute of Japan by the X-ray crystal density method using ^{28}Si-enriched spheres. For the realization, the volume of ^{28}Si-enriched spheres is measured by optical interferometry. The sphere surface characterization by X-ray photoelectron spectroscopy and ellipsometry is also performed. The relative standard uncertainty of the realization is estimated to be 2.4×10^{-8}. Details of the realization and future dissemination of mass standards in Japan based on the ^{28}Si-enriched spheres are described.

Keywords: Kilogram; Planck constant; New SI; Mass standards

1. Introduction

On May 20, 2019, the International System of Units (SI) was essentially revised. Presently, all SI units are defined in terms of the seven defining constants [1]. In the new SI, the kilogram, the unit of mass, is defined by fixing the value of the Planck constant. Under the new definition, it is in principle possible for each national metrology institute to realize the kilogram independently. To ensure the consistency among the realizations by national metrology institutes, an international comparison of the realizations based on the new definition, CCM.M-K8.2019, is presently organized by the Consultative Committee for Mass and Related Quantities. This comparison is an essential step to the dissemination of the kilogram based on the individual realization by each national metrology institute [2].

There are currently two independent methods that are capable of realizing the definition of the kilogram with relative uncertainties within a few parts in 10^8 [3]. The first of these relies on determining the unknown mass using an electromechanical balance specially designed for the purpose. The second method compares the unknown mass to the mass of a single atom of a specified isotope by counting the number of atoms in a crystal, where the mass of the atom is well-known in terms of the Planck constant. The second method is referred to as the X-ray crystal density (XRCD) method. After the confirmation of the international consistency of the realizations, the National Metrology Institute of Japan (NMIJ) will realize the kilogram on the basis of the new definition by the XRCD method. This method realizes the kilogram at a nominal mass of 1 kg using ^{28}Si-enriched spheres [4, 5]. Details of the realization at NMIJ and future dissemination of mass standards in Japan based on the ^{28}Si-enriched spheres are described in this paper.

2. X-ray Crystal Density (XRCD) Method

In the XRCD method, the number N of Si atoms in a Si sphere is counted by measuring its volume V_S and lattice constant a [4, 5]. The number N is given by

$$N = 8V_S/a^3, \quad (1)$$

where 8 is the number of atoms per unit cell of crystalline silicon. The mass of the sphere m_S is therefore expressed by

*Corresponding author, E-mail: n.kuramoto@aist.go.jp

$$m_s = Nm(\mathrm{Si}), \tag{2}$$

where m(Si) is the mass of a single Si atom. The new definition of the kilogram is based on the Planck constant h. The relationship between the Planck constant h and the mass of a single electron m(e) is given by

$$R_\infty = \frac{m(\mathrm{e})c\alpha^2}{2h}, \tag{3}$$

where c is the speed of light in vacuum, α is the fine-structure constant and R_∞ is the Rydberg constant [6]. The mass of a single Si atom m(Si) is related to m(e) by

$$\frac{A_r(\mathrm{Si})}{A_r(\mathrm{e})} = \frac{m(\mathrm{Si})}{m(\mathrm{e})}, \tag{4}$$

where A_r(e) and A_r(Si) are the relative atomic masses of electron and Si, respectively. Silicon has three stable isotopes, ^{28}Si, ^{29}Si and ^{30}Si. The value of A_r(Si) can therefore be determined by measuring the isotopic amount-of-substance fraction of each isotope. The relationship between m(Si) and h is given by

$$\frac{h}{m(\mathrm{Si})} = \frac{1}{2}\frac{A_r(\mathrm{e})}{A_r(\mathrm{Si})}\frac{\alpha^2 c}{R_\infty}. \tag{5}$$

By combining Eqs. (1), (2) and (5), we can express the sphere mass m_s in terms of h using

$$m_s = \frac{2R_\infty h}{c\,\alpha^2}\frac{A_r(\mathrm{Si})}{A_r(\mathrm{e})}\frac{8V_s}{a^3}. \tag{6}$$

Equation (6) is established when the Si sphere consists of only Si crystal. However, the surface of Si spheres is covered by a surface layer mainly consisting of amorphous SiO_2 [7]. Figure 1 shows the surface model of 1 kg ^{28}Si-enriched spheres manufactured from a silicon crystal highly enriched with the ^{28}Si isotope produced by the International Avogadro Coordination (IAC) project [8]. This surface model under vacuum was derived on the basis of surface characterization using various analysis techniques developed by the IAC project [7, 8]. In addition to the oxide layer (OL), a chemisorbed water layer (CWL) and a carbonaceous layer (CL) are also present. The CWL is a chemically absorbed water layer that remains under high vacuum conditions. The CL is a carbonaceous contamination layer formed by different adsorbed gases and contaminants, stemming from the environment during the measurement, handling, storage and cleaning of the sphere. These layers are hereinafter referred to as the surface layer (SL). Equation (6) should therefore be modified to

$$m_{\mathrm{core}} = \frac{2R_\infty h}{c\,\alpha^2}\frac{A_r(\mathrm{Si})}{A_r(\mathrm{e})}\frac{8V_{\mathrm{core}}}{a^3} - m_{\mathrm{deficit}}, \tag{7}$$

where m_{core} and V_{core} are the mass and volume of the "Si core" part, which excludes the surface layer, respectively, and m_{deficit} is the effect of point defects (i.e., impurities and self-point defects in the crystal) on the core mass [9]. The mass of the sphere m_{sphere} including the mass of the surface layer m_{SL} is given by

$$m_{\mathrm{sphere}} = m_{\mathrm{core}} + m_{\mathrm{SL}}. \tag{8}$$

The relative uncertainty of $R_\infty/(\alpha^2 A_r(\mathrm{e}))$ is estimated to be 4.0×10^{-10} [10] and the values of h and c are exactly defined in the new SI [1]. The values of a, A_r(Si) and m_{deficit} of the two 1 kg ^{28}Si-enriched spheres, AVO28-S5c and AVO28-S8c, were already measured by the IAC project with relative undercities at the level of 10^{-9} [9, 11], and it is confidently believed that these parameters are constant over the years. There is no known mechanism that changes those parameters when the Si crystal is kept close to room temperature. The kilogram can therefore be realized by measuring V_{core} and m_{SL} of the ^{28}Si-enriched spheres at NMIJ [4, 5]. Details of the measurements for the realization are described in the following sections.

3. Procedure of Realization of the Kilogram at NMIJ

The two ^{28}Si-enriched spheres, AVO28-S5c and AVO28-S8c, used for the realization of the kilogram at NMIJ were manufactured by the IAC project. The masses of the spheres are almost 1 kg, and details of the spheres are described in [8, 9].

To measure the sphere core volume V_{core} in Eq. (7), an optical interferometer for measuring the sphere diameter is used. However, the diameter measured by the optical

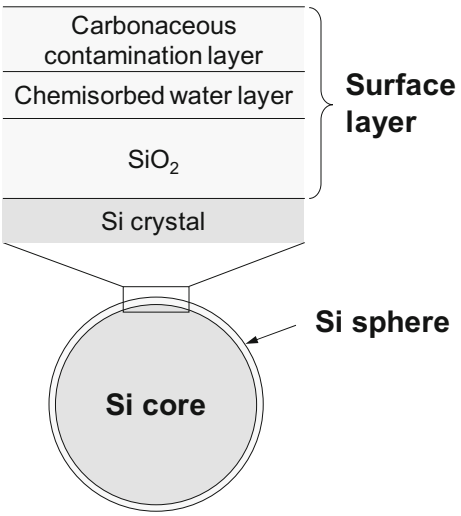

Fig. 1 Model of the surface layer of ^{28}Si spheres in vacuum derived by the IAC project [4, 5, 7]. In addition to the oxide layer (SiO_2), a chemisorbed water layer and a carbonaceous contamination layer are also present

interferometer is slightly different from the core diameter owing to the surface layer shown in Fig. 1. To calculate the core diameter from the measured diameter, the thickness of the surface layer is required. For the thickness measurement, an X-ray photoelectron spectroscopy (XPS) system and a spectroscopic ellipsometer are used. The surface mass, m_{SL} in Eq. (8), is derived from the surface characterization. Details of each measurement apparatus are presented in the following sections.

3.1. Sphere Volume Measurement by Optical Interferometry

Figure 2 shows a schematic drawing of the optical interferometer used to determine the volume of the ^{28}Si-enriched sphere by optical frequency tuning [12, 13]. A ^{28}Si-enriched sphere is placed in a fused-quartz Fabry–Perot etalon. The sphere and etalon are installed in a vacuum chamber equipped with an active radiation shield to control the sphere temperature. The pressure in the chamber is reduced to 10^{-2} Pa. Two beams (Beam 1 and Beam 2) from an external cavity diode laser are irradiated onto the sphere from opposite sides of the etalon. The light beams reflected from the inner surface of the etalon plate and the adjacent surface of the sphere interfere to produce concentric circular fringes. These are projected onto CCD cameras. The fractional fringe order of interference for the gaps between the sphere and the etalon, d_1 and d_2, are measured by phase-shifting interferometry [14, 15]. The sphere diameter D is calculated as $D = L - (d_1 + d_2)$, where L is the etalon spacing. To determine L, the sphere is removed from the light path by a lifting device installed underneath the sphere, and Beam 1 is interrupted by a shutter. Beam 2 passes through a hole in the lifting device, and the beams reflected from the two etalon plates produce fringes on a CCD camera. The fringes are also analyzed by phase-shifting interferometry. The sphere volume is determined from the mean diameter calculated on the basis of the diameter measurement from many different directions. The phase shifts required for phase-shifting interferometry are produced by changing the optical frequency of the diode laser. The optical frequency is controlled on the basis of the optical frequency comb, which is used as the national length standard of Japan [16, 17]. Details on the volume measurement are given in [12–14].

The temperature of the sphere is measured using small platinum resistance thermometers (PRTs) inserted into copper blocks that come in contact with the sphere. The copper blocks are coated with polyether ether ketone (PEEK) to prevent damage of the silicon sphere. The PRTs are calibrated using temperature fixed points in ITS-90 [18]. The measured diameters are converted to those at

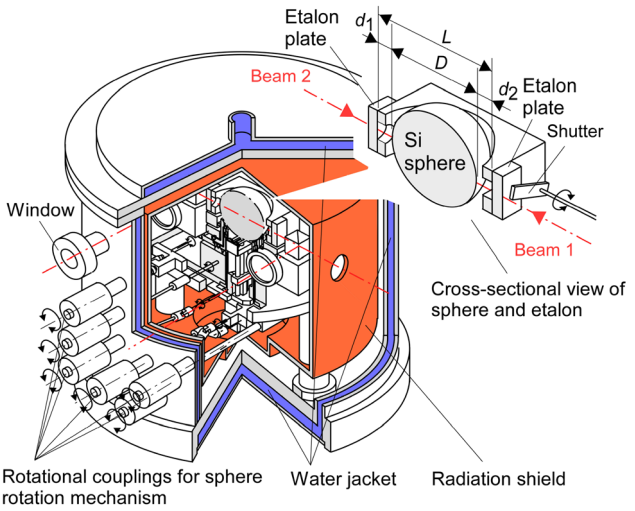

Fig. 2 Schematic drawing of the optical interferometer used to measure the volume of the ^{28}Si sphere. The ^{28}Si sphere and etalon are installed in a vacuum chamber equipped with an active radiation shield to control the sphere temperature. The uncertainty of the sphere temperature measurement is estimated to be 0.62 mK. Reused with the permission from IEEE [12]

20.000 °C using the thermal expansion coefficient of the enriched ^{28}Si-enriched crystal [19].

A sphere rotation mechanism installed under the sphere is used to measure the diameter from many different directions. In a set of diameter measurements, the diameter is measured from 145 directions distributed near-uniformly on the sphere surface [4]. Ten sets diameter measurement are performed, and between each set, the sphere is rotated to distribute the starting point of each set of measurements to the vertices of a regular dodecahedron. Because the ten directions defined by the vertices of a regular dodecahedron are uniformly distributed, the procedure therefore distributes all of the measurement points as uniformly as possible. The total number of the measurement directions is therefore 1450. The sphere volume is calculated from the mean diameter.

As an example of the results of the diameter measurement, the Mollweide map projection of the distribution of the diameter based on the 145 directions for AVO28-S5c is shown in Fig. 3 [4]. The three-dimensional plot of the diameter is displayed in Fig. 4, where the deviation from the mean diameter is enhanced.

A different type optical interferometer for the volume measurement of ^{28}Si-enriched spheres has been developed at the Physikalisch-Technische Bundesanstalt (PTB, Germany) [20]. Figure 5 shows a comparison of the mean diameters of a ^{28}Si-enriched sphere measured at PTB and NMIJ. In the interferometer developed at PTB, an etalon with spherical reference surfaces is used. The mean diameters obtained using the two interferometers with

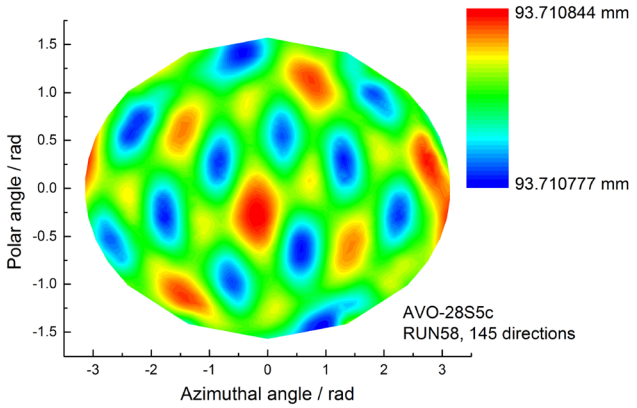

Fig. 3 Mollweide map projection of the distribution of the diameter based on 145 directions for AVO28-S5c. Reused with the permission from IEEE [4]

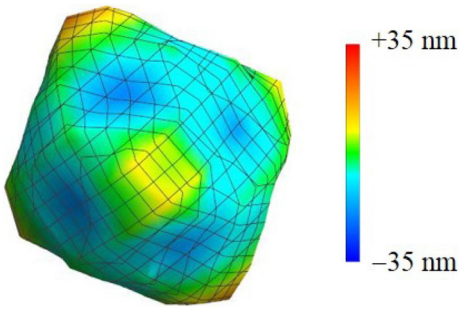

Fig. 4 Three-dimensional plot of the distribution of the diameter of AVO28-S5c. The peak-to-valley value of the diameter is 69 nm. Reused with the permission from IEEE [12]

different optical configurations and phase-shifting algorithms show excellent agreement within their uncertainties [12]. This shows the high reliability of the diameter and volume measurements at the two national metrology institutes.

3.2. Sphere Surface Characterization by XPS and Ellipsometry

X-ray photoelectron spectroscopy (XPS) and ellipsometry are used for the sphere surface characterization at NMIJ. The main component of the XPS system is ULVAC-Phi 1600C equipped with a monochromatic Al Kα X-ray source. The pressure in the XPS chamber is reduced to 5.0×10^{-7} Pa. A manipulator with a five-axis freedom is installed in the XPS chamber to realize the rotation of the sphere around the horizontal and vertical axes for the mapping of the entire surface. The sphere is placed on two rollers of the manipulator during the measurement. The rollers are made of polyimide for protecting the sphere

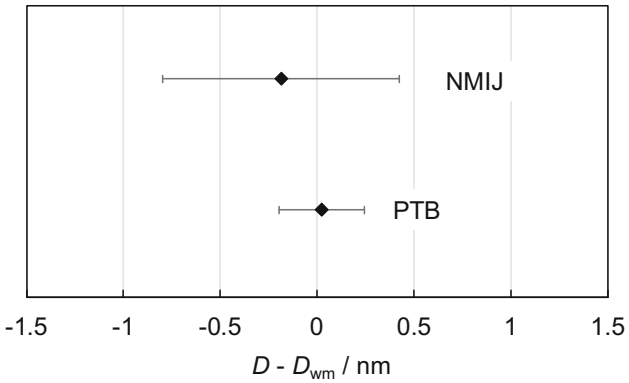

Fig. 5 Comparison of the mean diameters of a ^{28}Si-enriched sphere measured at PTB and NMIJ. The difference from the weighted mean diameter D_{wm} calculated from the diameters measured at the two national metrology institutes is plotted. The horizontal error bars indicate the standard uncertainty of each value. Reused with the permission from IEEE [12]

surface from damage during the rotation. Details of the XPS system are given in [21].

The main component of the spectroscopic ellipsometer is Semilab GES5E. Its spectral bandwidth ranges from 250 to 990 nm. The ellipsometer and an automatic sphere rotation system are integrated to a vacuum chamber to characterize the surface layer in vacuum, where the pressure is reduced to 1×10^{-3} Pa. The ellipsometric measurement can be carried out over the entire sphere surface using the automatic sphere rotation system. Details of the ellipsometer are provided in [22].

The thickness of the CL and OL at 52 points on the sphere surface is measured using the XPS system. The 52 points are distributed near-uniformly on the sphere surface [4]. The ellipsometer is used to examine the uniformity of the thickness of the OL at 812 points on the sphere surface [4].

Table 1 shows an example of the results of the surface characterization, where the thicknesses of all sublayers of AVO28-S5c measured in 2017 are tabulated. The thickness of the CWL estimated from the water adsorption coefficient to silicon surface reported in our previous work [23] is also listed in this table. The total thickness of the surface layer is about 3 nm.

Table 1 Mass, thickness and density of each sublayer in vacuum of AVO28-S5c. Reused with the permission from IEEE [4]

Layer	Thickness/nm	Density/g cm^{-3}	Mass/μg
OL	1.24(9)	2.2(1)	75.2(6.3)
CL	1.27(12)	1.08(14)	37.7(5.9)
CWL	0.28(8)	1.0(1)	7.7(2.3)
SL			120.6(8.9)

3.3. Mass of Surface Layer

The mass of the surface layer m_{SL} is given by

$$m_{SL} = m_{OL} + m_{CL} + m_{CWL}, \quad (9)$$

where m_{OL}, m_{CL} and m_{CWL} are the masses of the OL, CL and CWL, respectively. The masses are calculated from the thickness and density of each sublayer. The masses of all sublayers of AVO28-S5c measured in 2017 [4] are summarized in Table 1 with the density and thickness of each sublayer. The mass of the surface layer was determined to be about 120 μg with an uncertainty of 8.9 μg.

3.4. Volume of Si Core

The volume measured by the optical interferometer is slightly different from the core volume owing to the surface layer shown in Fig. 1. To determine the Si core volume, the total phase retardation on reflection at the sphere surface δ is calculated from the thickness and optical constants of each sublayer on the basis of the procedure in [14]. The value of δ is slightly smaller than π, and the effect of this phase shift on the gap measurement Δd is calculated using $\Delta d = \lambda\,(\delta - \pi)/(4\pi)$. This means that the actual diameter D_{actual} including the surface layer is larger than the apparent diameter measured by optical interferometry D_{app} by $-2\Delta d$. The phase shift correction to obtain the Si core diameter from the apparent diameter, Δd_0, was determined using $\Delta d_0 = -(2\Delta d + d_{total})$, where d_{total} is the sum of the thicknesses of all sublayers. The Si core diameter D_{core} is determined using $D_{core} = D_{app} + \Delta d_0$.

3.5. Mass Deficit

Owing to point defects and impurities, there is a mass difference between a sphere having Si atoms occupying all regular sites and the real sphere [9]. The mass difference, $m_{deficit}$ in Eq. (7), is given by

$$m_{deficit} = V_{core} \sum_i (m_{28} - m_i) N_i, \quad (10)$$

where m_{28} and m_i are the mass of a ^{28}Si atom and that of the point defect named i, respectively. For a vacancy, $m_i = m_v = 0$. For interstitial point defects, m_i is the sum of the masses of the defect and a ^{28}Si atom. N_i is the concentration of the point defect i. For example, $m_{deficit}$ of AVO28-S5c was estimated to be 3.6(3.6) μg [9].

3.6. Mass of Si Sphere

The sphere mass m_{sphere} is derived by using Eqs. (7) and (8) from the Planck constant, realizing the new definition of the kilogram. As an example, the uncertainty budget of the determination of m_{sphere} using AVO28-S5c in 2017 is shown in Table 2 [4]. This determination was performed for a pilot study to compare the realizations of the kilogram by several national metrology institutes on the basis of the Planck constant in CODATA 2014 [24]. The values of a and A_r(Si) of AVO28-S5c were measured with relative uncertainties of 1.8×10^{-9} and 5.4×10^{-9}, respectively, by the IAC project [9, 11]. The relative uncertainty of m_{sphere} was 2.4×10^{-8}. From this result, the relative uncertainty of the realization of the new kilogram is therefore estimated to be 2.4×10^{-8}, corresponding to 24 μg for 1 kg.

The largest uncertainty source for the realization is the sphere volume determination by optical interferometry, as shown in Table 2. For the more accurate realization at NMIJ, the optical interferometer is being improved [12]. This improvement will reduce the relative uncertainty of the realization of the kilogram will be reduced to 1.7×10^{-8}, corresponding to 17 μg for 1 kg.

4. Dissemination of the Mass Unit Based on the ^{28}Si-Enriched Spheres

Figure 6 shows the traceability chain of mass standards planned at NMIJ after the consistency of individual realizations of the kilogram by national metrology institutes is confirmed. The masses of the ^{28}Si-enriched spheres are determined by the XRCD method on the basis of the Planck constant as described in the previous sections. On the basis of the masses of the ^{28}Si-enriched spheres, the masses of 1 kg platinum–iridium weights and 1 kg stainless steel weights in air and vacuum are determined. These 1 kg weights will form an ensemble of reference mass standards and maintain the value of the realized kilogram at NMIJ.

The mass differences between the ^{28}Si-enriched spheres and the 1 kg weights are measured by using a mass comparator installed in a vacuum chamber, which enables mass comparisons at a constant atmospheric pressure or under vacuum [25]. Owing to density differences among silicon, stainless steel and platinum–iridium, the ^{28}Si-enriched spheres and the 1 kg weights have different volumes. This requires air buoyancy corrections in the mass difference measurement. For the precise air buoyancy correction, artifacts are used to accurately determine the air density [26]. The artifacts are a pair of weights that are equal in mass and surface area but different in volume. Furthermore, the masses of the ^{28}Si-enriched spheres and the 1 kg weights in air and those under vacuum are different owing to the difference in the amount of adsorbed water onto their surfaces. For the precise estimation of this sorption effect, a

Table 2 Uncertainty budget for the realization of the new kilogram by the XRCD method using AVO28-S5c at NMIJ. Reused with the permission from IEEE [4]

Uncertainty source	Relative standard uncertainty in m_{sphere}
Core volume, V_{core}	2.0×10^{-8}
Mass of the surface layer, m_{SL}	8.9×10^{-9}
Relative atomic mass of silicon, A_{r}(Si)	5.4×10^{-9}
Lattice parameter, a	5.5×10^{-9}
Mass deficit due to impurities and vacancies, m_{deficit}	3.8×10^{-9}
Relative combined standard uncertainty	2.4×10^{-8}

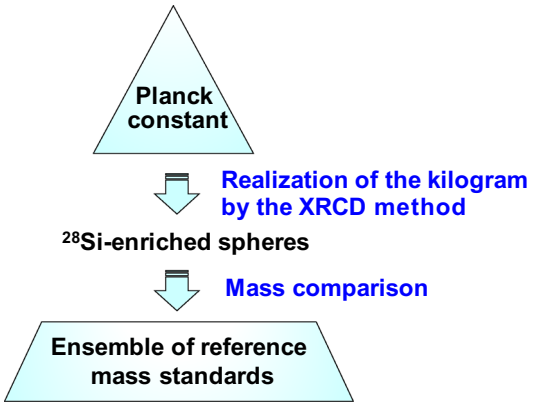

Fig. 6 Traceability chain from the new definition of the kilogram planned at NMIJ

pair of weights that are equal in mass and volume but different in surface area are used [27].

5. Small Mass Measurement Based on the Planck Constant

Under the previous definition of the kilogram, the metrological traceability of mass measurements was secured by using standard weights whose masses were measured on the basis of the international prototype of the kilogram. However, obtaining a standard weight with a mass less than 1 kg usually requires submultiples of a primary 1 kg standard. Each time a mass is subdivided, the relative uncertainty of the mass of the weights calibrated by the subdivision process accrues progressively.

On the other hand, the new definition enables us to realize the kilogram using any measurement technique that relates the Planck constant to the kilogram [3]. Mass in any range can therefore be directly measured on the basis on the definition of the kilogram without using the standard weights. An example of such measurement techniques is the use of an electrostatic force balance for mass measurements in mg range [28]. In this technique, electrostatic force is generated and is balanced with the gravity force acting on a sample, where the electrostatic force is measured on the basis of the Planck constant and the elementary charge. The electrostatic force balance can therefore realize the kilogram in the new SI [1] without using the standard weights. Recently, Shaw et al., have extended the measurement range by this technique to μg range [29]. At NMIJ, Yamamoto et al. have developed an electrostatic force balance for mass measurements in sub-mg range [30]. This balance will be also used for the realization of the kilogram at NMIJ in the future.

6. Conclusion

Under the new definition of the kilogram based on the Planck constant, it is in principle possible for each national metrology institute to realize the kilogram independently. After the confirmation of the international consistency of the individual realizations by national metrology institutes, NMIJ will realize the new kilogram by the XRCD method, where two ^{28}Si-enriched spheres manufactured by the International Avogadro Coordination project are used. The masses of the two spheres are almost 1 kg, and the relative standard uncertainty of the realization is estimated to be 2.4×10^{-8}, corresponding to 24 μg for 1 kg. On the basis of the spheres, the masses of weights consisting of the NMIJ ensemble of reference mass standards are measured. The ensemble will be used for dissemination of mass standards to scientific and industrial fields in Japan.

Acknowledgements This research work was partly supported by JSPS KAKENHI Grant Numbers 24360037, 16H03901 and 20H02630.

References

[1] The International System of Units (SI), 9th edition, Bureau International des Poids et Mesures (2019) https://www.bipm.org/utils/common/pdf/si-brochure/SI-Brochure-9-EN.pdf.

[2] CCM detailed note on the dissemination process after the redefinition of the kilogram, https://www.bipm.org/utils/common/pdf/CC/CCM/CCM_Note-on-dissemination-after-redefinition.pdf.

[3] Mise en pratique for the definition of the kilogram in the SI, https://www.bipm.org/utils/en/pdf/si-mep/SI-App2-kilogram.pdf .

[4] N. Kuramoto, L. Zhang, S. Mizushima, K. Fujita, Y. Azuma, A. Kurokawa and K. Fujii, Realization of the kilogram based on the Planck constant at NMIJ, IEEE Trans. Instrum. Meas., **66** (2017) 1267–1274.

[5] K. Fujii, H. Bettin, P. Becker, E. Massa, O. Rienitz, A. Pramann, A. Nicolaus, N. Kuramoto, I. Busch and M. Borys, Realization of the kilogram by the XRCD method, Metrologia, **53** (2016) A19–A45.

[6] P. Cladé, F. Biraben, L. Julien, F. Nez and S. Guellati-Khelifa, Precise determination of the ratio h/m_u: a way to link microscopic mass to the new kilogram, Metrologia, **53** (2016) A75–A82.

[7] I. Busch, Y. Azuma, H. Bettin, L. Cibik, P. Fuchs, K. Fujii, M. Krumrey, U. Kuetgens, N. Kuramoto and S. Mizushima, Surface layer determination for the Si spheres of the Avogadro project, Metrologia, **48** (2011) S62–S82.

[8] B. Andreas, Y. Azuma, G. Bartl, P. Becker, H. Bettin, M. Borys, I. Busch, P. Fuchs, K. Fujii, H. Fujimoto, E. Kessler, M. Krumrey, U. Kuetgens, N. Kuramoto, G. Mana, E. Massa, S. Mizushima, A. Nicolaus, A. Picard, A. Pramann, O. Rienitz, D. Schiel, S. Valkiers, A. Waseda and S. Zakel, Counting the atoms in a ^{28}Si crystal for a new kilogram definition, Metrologia, **48** (2011) S1–S13.

[9] Y. Azuma, P. Barat, G. Bartl, H. Bettin, M. Borys, I. Busch, L. Cibik, G. D'Agostino, K. Fujii, H. Fujimoto, A. Hioki, M. Krumrey, U. Kuetgens, N. Kuramoto, G. Mana, E. Massa, R. Meeß, S. Mizushima, T. Narukawa, A. Nicolaus, A. Pramann, S. A. Rabb, O. Rienitz, C. Sasso, M. Stock, R. D. Vocke Jr, A. Waseda, S. Wundrack and S. Zakel, Improved measurement results for the Avogadro constant using a ^{28}Si-enriched crystal, Metrologia, **52** (2018) 360–375.

[10] CODATA International recommended 2018 values of the Fundamental Physical Constants, https://physics.nist.gov/cuu/Constants/index.html.

[11] G. Bartl, P. Becker, B. Beckhoff, H. Bettin, E. Beyer, M. Borys, I. Busch, L. Cibik, G. D'Agostino, E. Darlatt, M. Di Luzio, K. Fujii, H. Fujimoto, K. Fujita, M. Kolbe, M. Krumrey, N. Kuramoto, E. Massa, M. Mecke, S. Mizushima, M. Müller, T. Narukawa, A. Nicolaus, A. Pramann, D. Rauch, O. Rienitz, C. P. Sasso, A. Stopic, R. Stosch, A. Waseda, S. Wundrack, L. Zhang and X. W. Zhang, A new ^{28}Si single crystal: counting the atoms for new kilogram definition, Metrologia, **54** (2017) 693–715.

[12] N. Kuramoto, L. Zhang, K. Fujita, S. Okubo, H. Inaba and K. Fujii, Volume measurement of a ^{28}Si-enriched sphere for a determination of the Avogadro constant at NMIJ, IEEE Trans. Instrum. Meas., **68** (2019) 1913–1920.

[13] N. Kuramoto, S. Mizushima, L. Zhang, K. Fujita, Y. Azuma, A. Kurokawa, S. Okubo, H. Inaba and K. Fujii, Determination of the Avogadro constant by the XRCD method using a ^{28}Si-enriched sphere, Metrologia, **54** (2017) 716–729.

[14] N. Kuramoto, K. Fujii and K. Yamazawa, Volume measurements of ^{28}Si spheres using an interferometer with a flat etalon to determine the Avogadro constant, Metrologia, **48** (2011) S83–S95.

[15] B. Andreas, L. Ferroglio, K. Fujii, N. Kuramoto and G. Mana, Phase corrections in the optical interferometer for Si sphere volume measurements at NMIJ, Metrologia, **48** (2011) S104–S111.

[16] H. Inaba, Y. Daimon, F. L. Hong, A. Onae, K. Minoshima, T. R. Schibli, H. Matsumoto, M. Hirano, T. Okuno, M. Onishi and M. Nakazawa, Long-term measurement of optical frequencies using a simple, robust and low-noise fiber based frequency comb, Opt. Express **14** (2006) 5223–5231.

[17] H. Inaba, Y. Nakajima, F. L. Hong, K. Minoshima, J. Ishikawa, A. Onae, H. Matsumoto, M. Wouters, B. Warrington and N. Brown, Frequency measurement capability of a fiber-based frequency comb at 633 nm, IEEE Trans. Instrum. Meas., **58** (2009) 1234–1240.

[18] H. Preston-Thomas, The international temperature scale of 1990 (ITS-90), Metroloiga, **27** (1990) 3–10.

[19] G. Bartl, A. Nicolaus, E. Kessler, R. Shödel and P. Becker, The coefficient of thermal expansion of highly enriched ^{28}Si, Metrologia, **48** (2011) S104–S111.

[20] A. Nicolaus, G. Bartl, A. Peter, E. Kuhn and T. Mai, Volume determination of two spheres of the new ^{28}Si-crystal of PTB, Metrologia, **54** (2017) 512–515.

[21] L. Zhang, N. Kuramoto, Y. Azuma, A. Kurokawa and K. Fujii, Thickness measurements of oxide and carbonaceous layer on a ^{28}Si sphere by using XPS, IEEE Trans. Instrum. Meas., **66** (2017) 1297–1303.

[22] K. Fujita, N. Kuramoto, Y. Azuma, S. Mizushima and K. Fujii, Surface layer analysis of a ^{28}Si-enriched sphere both in vacuum and in air by ellipsometry, IEEE Trans. Instrum. Meas., **66** (2017) 1283–1288.

[23] S. Mizushima, Determination of the amount of gas adsorption on SiO_2/Si(100) surfaces to realize precise mass measurement, Metrologia, **41** (2004) 137–144.

[24] M. Stock, P. Barat, P. Pinot, F. Beaudoux, P. Espel, F. Piquemal, M. Thomas, D. Ziane, P. Abbott, D. Haddad, Z. Kubarych, J. R. Pratt, S. Schlamminger, K. Fujii, K. Fujita, N. Kuramoto, S. Mizushima, L. Zhang, S. Davidson, R. G. Green, J. Liard, C. Sanchez, B. Wood, H. Bettin, M. Borys, I. Busch, M Hämpke, M. Krumrey and A. Nicolaus, A comparison of future realizations of the kilogram, Metroloiga, **55** (2018) T4–T7.

[25] S. Mizushima, N. Kuramoto, L. Zhang and K. Fujii, Mass measurement of ^{28}Si-enriched spheres at NMIJ for the determination of the Avogadro constant, IEEE Trans. Instrum. Meas., **66** (2017) 1275–1282.

[26] S. Mizushima, M. Ueiki and K. Fujii, Mass measurement of 1 kg silicon spheres to establish a density standard, Metrologia, **41** (2004) S68–S74.

[27] S. Mizushima, K. Ueda, A. Ooiwa and K. Fujii, Determination of the amount of physical adsorption of water vapour on platinum-iridium surfaces, Metrologia, **52** (2015) 522–527.

[28] G. Shaw, J. Stirling, J. A. Kramar, A. Moses, P. Abbot, R. Steiner, A. Koffman, J. R. Pratt and Z. Kubarych, Milligram

mass metrology using an electrostatic force balance, Metrologia, **53** (2016) A86–A94.
[29] G. A. Shaw, J. Stirling, J. Kramar, P. Williams, M. Spidell and R. Mirin, Comparison of electrostatic force and photon pressure force references at the nanonewton level, Metrologia, **56** (2019) 025002.
[30] Y. Yamamoto, K. Fujita and K. Fujii, Development of a new apparatus for SI traceable small mass measurements using the voltage balance method at NMIJ, IEEE Trans. Instrum. Meas. (2020). https://doi.org/10.1109/tim.2020.3001408.